Pure Appl. Chem., Vol. 83, No. 2, pp. 259–268, 2011.
doi:10.1351/PAC-CON-10-06-10

Atypical electric behavior of the double layer. Experimental case studies: Rh(111) in aqueous HCl solutions, and Au(111) in an ionic liquid, $BMIPF_6$*

Tamás Pajkossy

Institute of Materials and Environmental Chemistry, Chemical Research Center, Hungarian Academy of Sciences, Pusztaszeri út 59-67, Budapest H-1025, Hungary

Abstract: Cyclic voltammetry (CV), electrochemical impedance spectroscopy (EIS), and zero-charge-potential measurements have been performed for the title systems. The results of the Rh(111)/aqueous HCl solutions demonstrate that in solutions of binary electrolytes with adsorbing anions the interfacial impedance is a single, indivisible element, even if its frequency dependence implies a four-element circuit. The measurements on Au(111) in 1-butyl-3-methylimidazolium hexafluorophosphate ($BMIPF_6$) reveal that double-layer formation and rearrangement in ionic liquids are very slow processes manifesting themselves as a parallel combination of a capacitance and a constant phase element (CPE).

Keywords: electrochemistry; equivalent circuits; impedance; ionic liquids; single crystals.

INTRODUCTION

Double layers at electrode surfaces have always played a central role in electrochemistry, since their structure and the associated electric fields strongly affect the kinetics of chemical processes therein. The aim of the double-layer studies is the characterization of surface concentrations ("coverages") of electrolyte species, their distribution along the distance from electrode surface, and related issues. Surface concentrations can be determined by, or calculated from, measurements of many and diverse—various optical, spectroscopic, radiotracer, X-ray diffraction, quartz-crystal microbalance, and others—techniques; however, the electrical characterization of the interface has been and remains the most important experimental approach. This comprises the measurement of time-dependent currents as a function of time-dependent potentials (or contrariwise) and the representation of results in terms of time-independent quantities, like charges or capacitances. Accordingly, double-layer theories are tested by their predictions regarding the electrical behavior (mostly double-layer capacitance as a function of potential and electrolyte composition) rather than by those of the chemical composition of the interfacial region.

Both the theoretical and experimental double-layer studies—disregarding exceptions—always consider the absence of Faradaic processes; the underlying assumption is that Faradaic (i.e., those with steady-state charge transfer) and non-Faradaic (i.e., interface charging) processes are separable because they are independent of each other. Thus, the typical experiments with no Faradaic reactions for inves-

*Paper based on a presentation made at the 2nd Regional Symposium on Electrochemistry: South East Europe (RSE SEE-2), Belgrade, Serbia, 6–10 June 2010. Other presentations are published in this issue, pp. 253–358.

tigating the double layer are done with noble metals in electrolytes with appropriate conditions (electrolyte composition and electrode potential) for avoiding redox processes.

Double layers—from an electrical point of view—are condensers of voltage-dependent capacitances, the charging of which might be delayed by resistances. Accordingly, the usual modeling employs equivalent circuits of capacitors, resistors, and occasionally diffusion elements; the capacitive elements of the circuit represent spatially separated charge structures that are independent of each other. The subject of the present lecture/article is the demonstration of two cases when either the capacitances are coupled to each other or one element of the double layer is a constant phase element (CPE) rather than a capacitor. The two examples discussed are Rh(111) in aqueous hydrochloric acid and Au(111) in a room-temperature ionic liquid, 1-butyl-3-methylimidazolium hexafluorophosphate ($BMIPF_6$). These measurements have already been published; for experimental details, see refs. [1,2].

RELEVANT CONCEPTS AND RELATED METHODS

Having an electrochemical cell, we have the possibility of controlling voltage across its terminals and to measure voltages and currents, as a function of time, t. Most often, potentiostatic arrangement is used, that is, the $E(t)$ electrode potential is controlled and the $I(t)$ current is measured. In what follows, we assume that no Faradaic processes proceed, thus the role of the current is to charge/discharge the interface. Understanding double-layer structure means first of all the determination of surface concentrations (surface excesses, coverages) of solution species; the relevant first point concerns how we can transform the surface-area normalized $I[t,E(t)]$ data to surface excesses. In principle, it is done in three steps.

First, the time-dependent data are transformed into time-independent ones: specifically, the capacitance, $C(E)$, is determined. Secondly, provided that a charge zero point is known, surface charge [that is, of excess electrons on metal, $q^{\mathrm{M}}(E)$] is calculated by integrating capacitance with potential, respectively. In the third—perhaps the most intricate—step, charges are converted to surface concentrations using the formal partial charge number (electrosorption valency) as one proportionality factor. We shall not deal with this step, instead, we use the frequently applied approximation for ion adsorption: this factor will be regarded to be the same as the charge number, z, of the adsorbate.

The first and second steps involve the experimental techniques of determination of capacitance (by electrochemical impedance spectroscopy, EIS, sometimes by cyclic voltammetry, CV) and potential of zero charge, respectively. These techniques are summarized in the next two sections.

DETERMINATION OF THE CAPACITANCE

Double-layer capacitance is determined by various types of measurements all employing voltage or current perturbations. Irrespective of the type of perturbations (steps, pulses, sine waves, noise, etc.), in fact, these all are impedance measurements. The traditional way of single-frequency capacitance measurements—when potential is scanned slowly and a small amplitude sinusoidal signal tests the capacitance, directly yielding the $C(E)$ curve—is correct only if the equivalent circuit of the electrode is a simple serial R_{S}–C_{S} one; otherwise it yields ambiguous results. Just because of this, capacitance has been determined in the past two to three decades mostly through measurements of impedance at multiple frequencies, that is, via EIS measurements.

The usual way of analyzing impedance spectra is to find an appropriate equivalent circuit, which reasonably represents the physico-chemical processes involved, then to fit the equivalent circuit's spectrum to the measured one by varying the circuit's parameters.

In the absence of Faradaic reactions, the low-frequency limit of the impedance is always of minus infinite imaginary value, and the spectrum, on the complex plane, looks like the one depicted in Fig. 1a. Such spectra can often be approximated by the equivalent circuit shown in Fig. 1b.

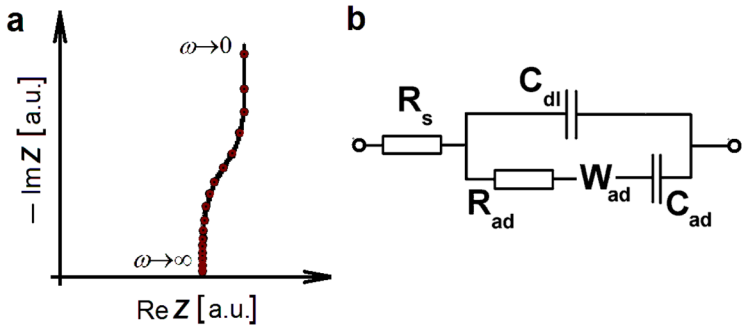

Fig. 1 Illustration of an impedance spectrum for electrochemical systems in the absence of Faradaic reactions (a) and corresponding equivalent circuit (b).

The origin of this equivalent circuit is the combination of the adsorption impedance models of Dolin and Ershler [3] and of Frumkin and Melik-Gaykazyan [4]. The electrode is assumed to be in contact with a solution comprising a base electrolyte of major concentration plus one adsorbate species of minor concentration. The equivalent circuit predicted by the theory has the following components: The series resistance, R_s, is a trivial property of the solution bulk; the single capacitance C_{dl}—representing the fast component of the double-layer charging—is interpreted as the electrostatic charging by the majority charge carriers; the R_{ad}–W_{ad}–C_{ad} branch corresponds to the adsorption of the minor component. The R_{ad} adsorption-rate-related and the W_{ad} diffusion-related terms—the latter having a $(i\omega)^{1/2}$ frequency dependence for planar geometry—are dominant if the rate of adsorption is small or high, respectively.

This equivalent circuit adequately and accurately represents the underlying physics and physicochemistry; moreover, it can also be used for the empirical description of certain other cases when the above conditions do not apply. Still, the two capacitances might be interpreted in the same way.

The $C(E)$ curve [depending on the interpretation, the $C_{dl}(E)$ or the $C_{ad}(E)$ curves] is determined by taking impedance spectra at various E potentials; the parameters of the above equivalent circuit (or of similar ones) are obtained by fitting to the measured spectra.

The usual complex-plane plot of impedance spectra of such capacitive systems, as the one in Fig. 1, is not really informative (the high-frequency part is compressed; the details there are invisibly small). Instead, it is more instructive to display the complex interfacial capacitance function, calculated as $C(\omega) = 1/i\omega(Z(\omega) - R_s)$. This transformation yields arc-shaped spectra on the complex plane; certain important parameters of the equivalent circuit are directly seen on such a plot (Fig. 2). The high- and low-frequency limits of the arc are C_{dl} and $C_{dl} + C_{ad}$, respectively; the shape reveals the kinetics of adsorption (whether or not diffusion plays a role); finally, as it can be shown, with increasing adsorbate concentration the spectrum points shift clockwise along the arc—thus a concentration dependence of spectra can help to identify the adsorbate.

Two additional points need to be mentioned.

(i) It often happens that the adsorption-related branch of the circuit cannot be resolved to the above three terms. For empirical description, this branch, or at least some elements of it, can be replaced by a two-parameter, single-impedance element, the CPE, defined by its admittance as $Y_{CPE}(\omega) = Q(i\omega)^n$ where Q and $0 < n < 1$ are the CPE coefficient and CPE exponent, respectively. The usual reason for the appearance of a CPE is that some process has a broad time constant distribution due to some sort of irregularity.

(ii) In special cases, capacitance can be determined from cyclic voltammograms by normalizing current by scan rate, v: $C_{dc} \equiv dq^M/dE = (dq^M/dt)/(dE/dt) = I/v$. Determined this way, it is named "dc-capacitance".

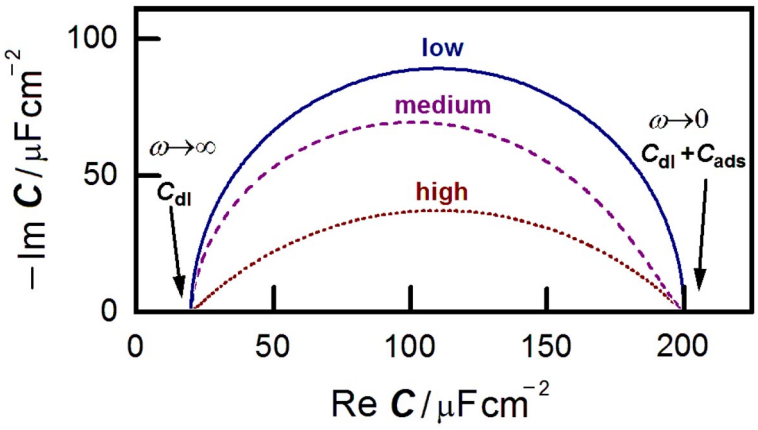

Fig. 2 Capacitance complex plane plots for the circuit of Fig. 1b with C_{dl} = 20 μF/cm^2 and C_{ad} = 180 μF/cm^2, for cases of high, medium, and low adsorption rate coefficients.

DETERMINATION OF THE POTENTIAL OF ZERO CHARGE

There are three different concepts (plus their combinations) that are some sort of conditions of electric neutrality, "zero charge potentials"; these three concepts imply (and are applied for) different conditions.

1. Consider an electrode immersed in dilute solution with inert ions. The double layer is formed as the joint effect of electrostatic forces and thermal motion: ions are attracted to (or repelled from) the electrode and are scattered by thermal motion. At a certain potential, at the potential of zero free charge, *pzfc*, close to the interface the charge of anions and cations is equal—accordingly, the electronic charge of the metal is zero. Such a situation can be identified—as with Hg electrodes in dilute NaF solutions [5]—if a sharp minimum is observed on the $C(E)$ in accord with the Gouy-Chapman theory [6,7].
2. Consider an electrode immersed in an electrolyte containing also ions that can be adsorbed on the electrode's surface. In this case, the electronic charge on the metal must compensate the charges bound to the surfaces both by adsorption and electrostatic forces. Accordingly, at the potential of zero total charge, *pztc*, the electronic charge of the metal is zero; the sum of all ionic charges (adsorbed plus electrostatically bound) on the solution side is also zero. Since in this case the situation is governed by chemical rather than by electrostatic forces, no theory—based solely on classical physics—can predict the *pztc*.

   However, *pztc* is a measurable quantity: by measuring the charge during creation, or during the elimination of the double layer. For the former measurement, assume that the metal and the electrolyte are separated from each other, while a certain voltage is maintained between them. Technically this can be done, as Fig. 3 illustrates, by immersing the electrode in the electrolyte with a connected potentiostat applying a steady potential E. Just at the moment of immersion, the double layer is formed whose charge is provided by the potentiostat in the form of a current transient—the charge of which is zero just at the *pztc*. Such a measurement [8] is very simple in principle, in practice it is difficult because the metal surface must be completely oxide-free.

   The alternative is the charge measurement during elimination of the double layer, like the CO charge displacement measurement elaborated for platinum [9] and other platinum group metals [10]. Initially, the platinum electrode is kept at some E potential, at which CO is ready to be adsorbed without getting oxidized. If CO is bubbled through the solution, it is adsorbed on the Pt surface and replaces all adsorbed ions. Using the terms of electrostatics, by introducing a spacer

layer between the two arms of the condenser, the charge of the condenser is decreased, since the voltage is kept constant. Charge reduction appears as a current transient; this charge is zero just at the *pztc*.

Unfortunately, this double-layer elimination technique is available for a few systems only.

3. The third zero point refers to dipole rather than ion movements, in particular in aqueous solutions. Metal electrodes, unless fully covered by ionic adsorbates, are in contact with water, whose molecules are electric dipoles. The orientation of dipoles is affected by the electrode potential; at a certain potential the dipoles may flip over, as it was demonstrated on Pt(111) by capacitance measurements [11], and by laser-heating experiments [12]. The authors of the latter publication named the potential of the flip-over as potential of maximum entropy, *pme*.

The magnitudes of the three effects are different. The capacitances associated with the *pzfc* and the *pme* are smaller—even by one order of magnitude—than those related to adsorption; hence, the former capacitances can be observed in the rare, exceptional cases when adsorption capacitance is negligibly small or can be eliminated in some way.

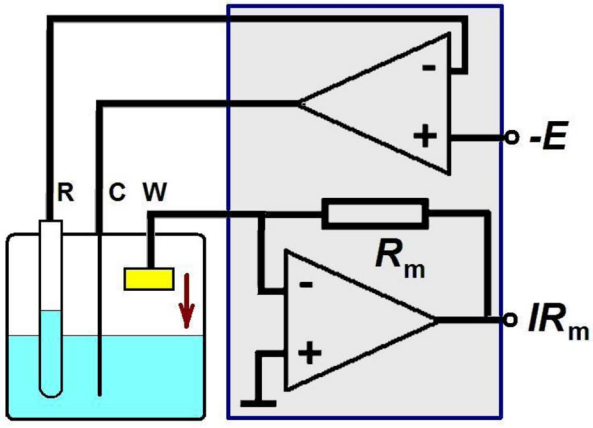

Fig. 3 Scheme of the *pztc* measurement. The potentiostat (in the gray box) is represented by its two main operational amplifiers, by the ones for potential control and for current-to-voltage conversion.

Rh(111) IN 0.1 M HCl

Rh(111) in 0.1 M HCl is an electrode for which ion adsorption dominates the dynamic behavior of the double layer. It is a very stable system; the potential can be cycled even for hours without significant change of its voltammogram (Fig. 4) within the given limits.

The voltammogram exhibits three important features: (i) there is a sharp peak around –0.23 V vs. SCE; (ii) the anodic and cathodic peaks are not mirroring each other, indicating slow processes; (iii) at potentials $E > 0.2$ V, the voltammogram is of very low current without features; this potential range—up to that of OH^- adsorption (not discussed here)—is a double-layer region.

The electrode's charge, q^M, calculated by integrating the voltammogram, is also displayed in Fig. 4. Note that *pztc* ($q^M = 0$) is just at the peak; negative and positive of the peak, q^M reaches the values of approximately –200 μC/cm^2 and around +120 μC/cm^2, implying adsorbed monolayers of adsorbed cations and anions—most probably hydrogen and chloride, respectively. Although these numbers give no clue to the chemical state of the adsorbed species (whether or not they are discharged), the charge values support the interpretation that the surface is always covered by a monolayer of an adsor-

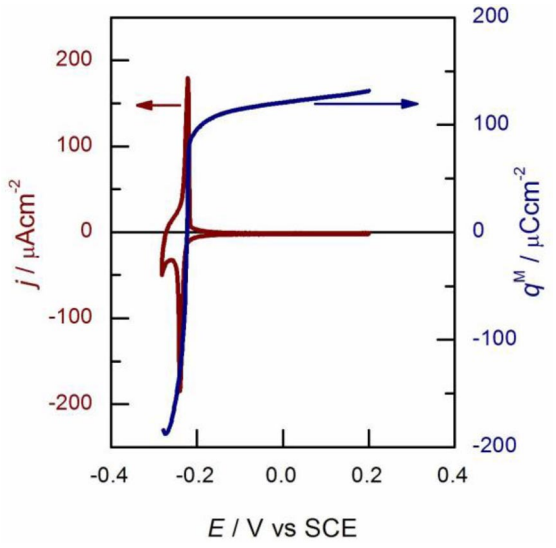

Fig. 4 CV and charge, $q^{M}(E)$ of Rh(111) in 0.1 M HCl at 10 mV/s. The $q^{M}(E)$ curve has been calculated by integration of the positive scan of the $j(t)$ curve using the *pztc* value of –0.22 V obtained from CO charge displacement measurement.

bate in the full potential range of Fig. 4; however, the composition of the monolayer is changed from hydrogen to chloride with increasing electrode potential.

Capacitance spectra, in the full potential range of Fig. 4, are arcs—single arcs in the double-layer region and double arcs in the region of the peak (Fig. 5). The single arcs *empirically* can be well fitted by the equivalent circuit of Fig. 1b; for fitting the double arcs, an additional RC branch had to be added in the equivalent circuit (inset of Fig. 5b).

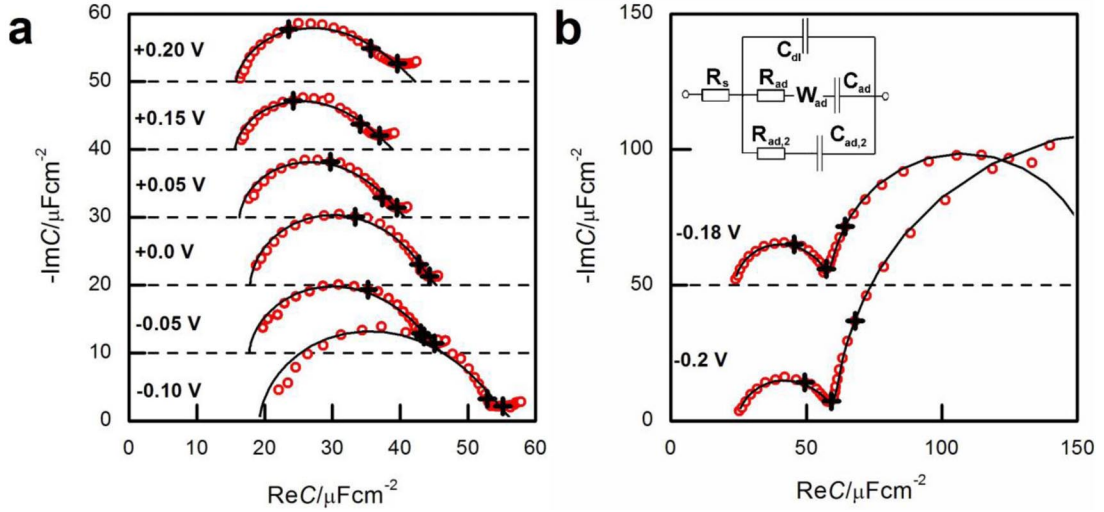

Fig. 5 Capacitance spectra (10 kHz–1 Hz) of Rh(111) in 0.1 M HCl at potentials of the double-layer region (a) and at the positive end of the adsorption peak (b). On the capacitance plots, the 1 kHz, 100 Hz, and 10 Hz points are indicated by crosses; solid lines are the fitted spectra. The spectra are shifted along the ordinate for visibility reasons. Inset of (b) is the equivalent circuit that models double-arc spectra.

For the identification of circuit elements, the spectra were measured with various KCl + HCl solutions. With increasing Cl^- concentration, the points of the single-arc spectra in the double-layer region (as those of Fig. 5a) and the high-frequency arcs of the double arcs shift clockwise, proving that the R_{ad}–W_{ad}–C_{ad} branch of the equivalent circuit corresponds to Cl^- adsorption. Accordingly, the $R_{ad,2}$–$C_{ad,2}$ branch models hydrogen adsorption.

The $C_{dl}(E)$ and $C_{ad}(E)$ functions run parallelly in a fairly broad potential range (Fig. 6), suggesting that charging of both capacitances involves the same species—in other words, the charges both at the outer and inner Helmholtz planes (OHP and IHP, respectively) are those of chloride ions. When chloride ions are moving from a point just outside the double layer to the adsorbed state, they first appear at the OHP corresponding to electrostatic charging; from there they may enter in the IHP, which is adsorption. Although represented by parallel C_{dl} and R_{ad}–W_{ad}–C_{ad} branches, double-layer charging and adsorption are sequential rather than parallel processes, and are not independent of each other. Such a coupling is analogous to the "Delahay's coupling" [13] prevailing if the same species takes part both in double-layer charging and Faradaic processes.

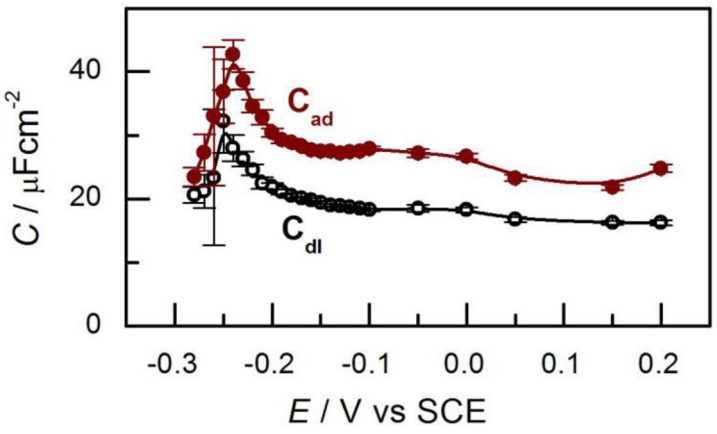

Fig. 6 Potential dependence of C_{dl} (open circles) and C_{ad} (solid circles).

Finally, the circuit elements R_{ad} and W_{ad} express the kinetics of chloride movement between outer and inner Helmholz planes: Evidently, W_{ad} has nothing to do with diffusion; it is an empirical element—its nature remains an open issue.

Because of the strong coupling of the two capacitances, and also taking into account that the R_{ad}–W_{ad} elements also express the chloride relocation in the double layer, the interfacial impedance should be regarded as a single, indivisible element rather than a four-element circuit.

Au(111) IN $BMIPF_6$

Ionic liquids are relatively new systems for electrochemists—there is no consensus even on their fundamental properties, like on their double-layer behavior. Just to do the basic characterization of a well-defined electrode in an often studied ionic liquid, we have performed the same three types of experiments as with the Rh(111)/HCl system: (a) CVs to characterize the system in general; (b) impedance spectra have been measured for the determination of interfacial capacitance; (c) finally, *pztc* was determined by immersion experiments. For the experimental details, see ref. [2]. These experiments yielded the following results:

(a) The polarizability range of ionic liquids is much larger than that of aqueous solutions; accordingly, in many instances of ionic liquids' CVs, various electrodes are presented that show a flat "double-layer"-type behavior over a range of 4 V and more. However, with increased current-metering sensitivities humps and peaks appear, which might be in connection with irreversible processes. There is a relatively narrow potential range only, in which potential can be cycled to yield a steady-state voltammogram. For the system studied, Au(111) in $BMIPF_6$, such a voltammogram is shown in Fig. 7. The two CVs are fairly stable and reproducible (at least for an hour or so); however, all features, including the P peak location, change with sweep rate even at 2 mV/s.

(b) Impedance spectra have been measured in this potential range; they all could be well modeled by the equivalent circuit shown as inset of Fig. 8a. Some spectra are shown in Fig. 8a in capacitance representation, whereas the potential dependence of C_{dl} and of the CPE parameters is presented in Fig. 8b.

The capacitance C_{dl} shows little if any potential dependence (Fig. 8b, crosses), its value is about 6–7 $\mu F/cm^2$. This low, potential-independent capacitance value is against the predictions of recent theories [14,15]. The CPE coefficient exhibits a peak around –0.3 V; whereas the CPE exponent shows some—although rather scattered—potential dependence.

(c) The *pztc* has been determined by the immersion technique*. In contrast to measurements in aqueous solutions when the current decays to zero, here the transients are power-law-like with time (in accord with the CPE behavior of impedance) and consequently, also the charge vs. time curves do not attain a steady value even in minutes (Fig. 9a). This is why the charges calculated with some arbitrary (100 s) integration time are used for plotting the charge vs. immersion potential plot (Fig. 9b). The zero-crossing (i.e., the *pztc*) is around –0.1 V vs. Ag/AgCl; the electronic charge of the metal is in the order of magnitude of 50–100 $\mu C/cm^2$ if the potential deviates from the *pztc* by about 0.5 V.

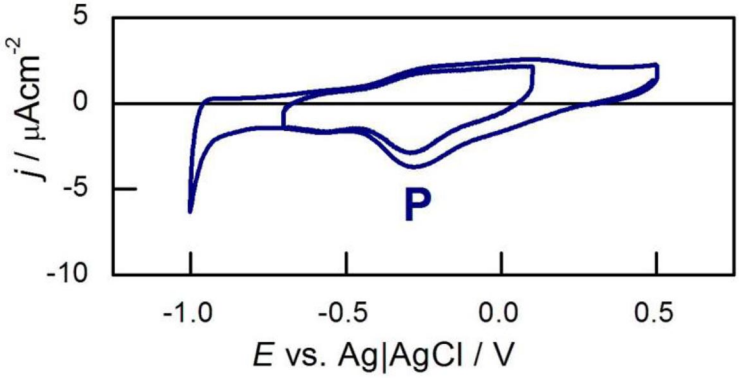

Fig. 7 CV of Au(111) in $BMIPF_6$ at 50 mV/s.

*This measurement was carried out by Mr. Markus Gnahm.

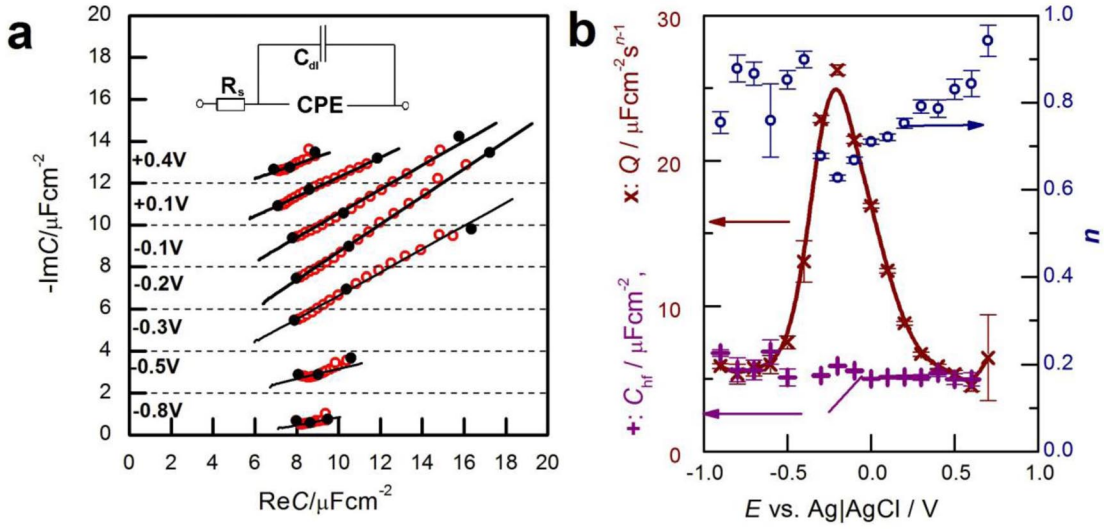

Fig. 8 (a) Impedance spectra at potentials (vs. Ag/AgCl) indicated, in capacitance representation. On the capacitance plots, the 100 Hz, 10 Hz, and 1 Hz points are indicated by full symbols; solid lines are the fitted curves using the equivalent circuit of the inset. The spectra are shifted along the ordinate for visibility reasons. (b) The fitted equivalent circuit parameters, as function of potential. C_{dl} (+), Q (x), and n (o) data obtained from fitting of the measured spectra (some of them are plotted in a). Note that C_{dl} and Q are of different dimensions.

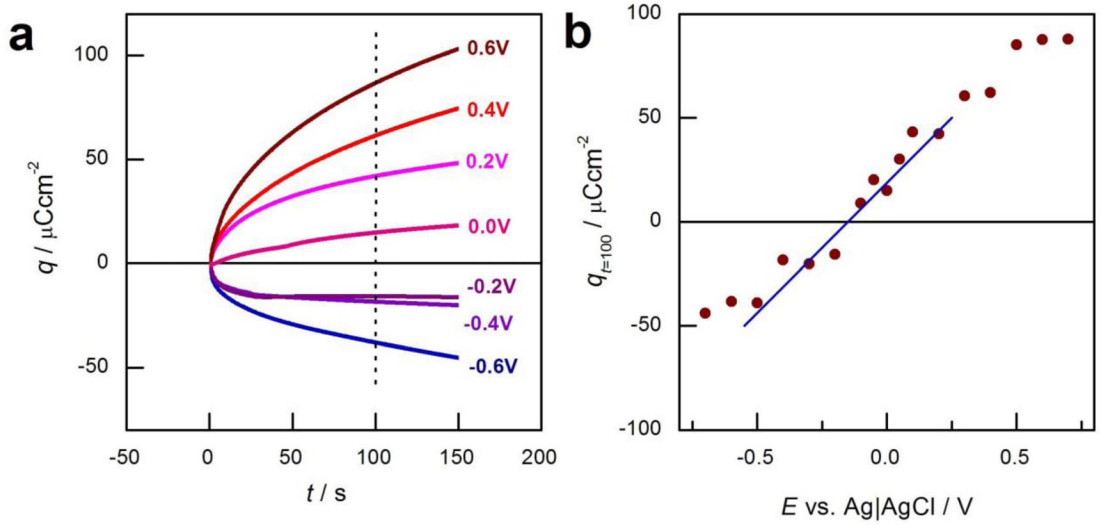

Fig. 9 (a) Integrated immersion current transients at potentials indicated; (b) the charge calculated for 100 s as function of potential.

We interpret the measurements as follows: First, the three potentials—the potential of peak P, of the CPE coefficient maximum, and of the zero-crossing of the immersion charge—are the same; the apparent differences being due to different "effective scan rates". We attribute this peak to the complete reorientation of the double layer: this is the potential, where the innermost ion layer changes its polarity. Negative and positive to the peak, the BMI^+ cations and the PF_6^- anions dominate the Helmholtz layer, respectively; concomitantly, the *pztc* is at the peak.

Secondly, the charging process in the studied potential range is much slower than with aqueous electrolytes: the CV changes shape by sweep rate change even at the 2 mV/s; the impedance is a CPE at 1 Hz; the immersion charge keeps increasing even after 2 min. This means that the time of formation/rearrangement of the interfacial layer is much longer than for aqueous electrolytes. Sluggish processes manifest themselves also in high viscosity and low ionic mobility.

Thirdly, since the measurements have been done with Au(111), interfacial irregularities as causes of CPE [16] can be safely excluded. In this case, the CPE is the manifestation of a broad time constant distribution: the ionic liquid is not a simple molecular liquid; charges are linked to each other, complete domains must be reorganized for any electric field change—such collective motions lead to broad time constant distributions.

CONCLUSIONS

Two simple electrochemical systems have been shown whose double-layer electric properties differ from those of textbook systems:

(i) In solutions of binary electrolytes with adsorbing anions [example: Rh(111)/aqueous HCl solutions] the interfacial impedance is a single, indivisible element, even if its frequency dependence implies a four-element circuit. Its indivisible nature is due to the fact that the one and the same species, the Cl^- ion, is the one that is at the OHPs and IHPS and moves between them.

(ii) Double-layer formation and rearrangement in ionic liquids [example: Au(111)/BMIPF_6] are very slow processes manifesting themselves as a parallel combination of a capacitance and a CPE.

ACKNOWLEDGMENTS

The author has made the experiments as a guest of the Institute of Electrochemistry, University of Ulm, Germany; he is indebted to Prof. Dr. Dieter M. Kolb and co-workers for hospitality, cooperation, help, and advice. The work has been funded by a bilateral agreement of the Deutsche Forschungsgemeinschaft, and the Hungarian Academy of Sciences. Financial support of the Hungarian Science Research Fund OTKA-NKTH (No. 67874) is acknowledged.

REFERENCES

1. T. Pajkossy, D. M. Kolb. *Electrochim. Acta* **54**, 3594 (2009).
2. M. Gnahm, T. Pajkossy, D. M. Kolb. *Electrochim. Acta* **55**, 6212 (2010).
3. P. Dolin, B. Ershler. *Acta Physicochim. URSS* **XIII**, 747 (1940).
4. A. N. Frumkin, V. I. Melik-Gaykazyan. *Dokl. Akad. Nauk.* **5**, 855 (1951).
5. D. C. Grahame. *Chem. Rev*. **41**, 441 (1947).
6. (a) G. Gouy. *J. Phys. Radium* **9**, 457 (1910); (b) G. Gouy. *Compt. Rend*. **149**, 654 (1910).
7. D. L. Chapman. *Philos. Mag.* **25**, 475 (1913).
8. U. W. Hamm, D. Kramer, R. S. Zhai, D. M. Kolb. *J. Electroanal. Chem.* **414**, 85 (1996).
9. J. Clavilier, R. Albalat, R. Gómez, J. M. Orts, J. M. Feliu. *J. Electroanal. Chem.* **360**, 325 (1993).
10. J. M. Orts, R. Gómez, J. M. Feliu, A. Aldaz, J. Clavilier. *Electrochim. Acta* **39**, 1519 (1994).
11. T. Pajkossy, D. M. Kolb. *Electrochim. Acta* **46**, 3063 (2001).
12. V. Climent, B. A. Coles, R. G. Compton. *J. Phys. Chem. B* **106**, 5988 (2002).
13. K. Holub, G. Tessari, P. Delahay. *J. Phys. Chem.* **71**, 2612 (1967).
14. K. B. Oldham. *J. Electroanal. Chem*. **613**, 131 (2008).
15. A. A. Kornyshev. *J. Phys. Chem. B* **111**, 5545 (2007).
16. T. Pajkossy. *Solid State Ionics* **176**, 1997 (2005).

